High-frequency gravity waves observed in the low-latitude mesosphere-lower thermosphere (MLT) region and their possible relationship to lower-atmospheric convection

S. Kovalam,[1] T. Tsuda,[2] and S. Gurubaran[3]

Received 12 January 2011; revised 31 March 2011; accepted 21 April 2011; published 2 August 2011.

[1] Observations of Medium Frequency (MF) radar winds made at Pameungpeuk (7.5°S, 107.5°E) and Tirunelveli (8.7°N, 78°E) between February and March 2010 are used to study gravity wave activity in the equatorial mesosphere and lower thermosphere (80–100 km). Gravity wave variances in the 20–120 min period band and their spectra are computed. Daily values of gravity wave variances show modulations on time scales ranging from diurnal to planetary waves. Spectra of wave variances display peaks at tidal periods and show evidence of gravity wave modulation at 24, 12, and 8 h periods. Statistical investigation of waves, made using Stokes parameter technique, indicates that the directionality of the mesospheric wave field is highly anisotropic. The role of lower-atmospheric sources on the MLT gravity wave variability is also examined. Spatial distribution of cloud top temperature and rainfall rates are used. GW activity at mesosphere-lower thermosphere (MLT) heights shows clear anticorrelation with the cloud top temperature and positive correlation with rainfall rates suggesting a possible link between observed gravity wave variability and the variations in the deep tropical convection.

Citation: Kovalam, S., T. Tsuda, and S. Gurubaran (2011), High-frequency gravity waves observed in the low-latitude mesosphere-lower thermosphere (MLT) region and their possible relationship to lower-atmospheric convection, *J. Geophys. Res.*, *116*, D15101, doi:10.1029/2011JD015625.

1. Introduction

[2] Gravity waves (GWs) are ubiquitous throughout the middle atmosphere. It is now well recognized that they play an important role in the overall dynamics of the middle atmosphere by partly determining the large-scale temperature and wind structure through their transportation of energy and momentum (see, e.g., reviews by *Fritts and Alexander* [2003]). The majority of the GWs arise in the lower atmosphere by disturbances such as storms, squall line, jet stream, orography and convection. GWs generated by tropical convection propagate vertically [e.g., *Holton and Alexander*, 1999], produce turbulence and deposit momentum and energy when breaking, thereby influencing the general circulation, thermal regime and composition of the middle atmosphere [e.g., *Andrews et al.*, 1987]. GWs are thought to be a major cause of variations in the mean zonal winds such as the quasi-biennial oscillation (QBO) in the lower and middle stratosphere [*Dunkerton*, 1997; *Baldwin et al.*, 2001]. They also appear to play an important role in driving the strong semiannual oscillations (SAO) in the mean zonal winds that occur in the altitude range 30–90 km over the equator. The largest SAO amplitudes (~30 ms^{-1}) occur near the mesopause (MSAO) [*Burrage et al.*, 1996; *Yoshida et al.*, 1999] and the stratopause (SSAO), with small amplitudes observed near 65 km [*Hirota*, 1978; *Hamilton*, 1982; *Garcia et al.*, 1997; *Garcia and Sassi*, 1999]. In particular, the MSAO is out of phase with the SSAO, which suggests that it is driven, in part, by GWs that are selectively filtered.

[3] Extensive climatological studies of GWs in the middle atmosphere have been conducted over past 40 years utilizing a variety of techniques, including MF radars [*Reid and Vincent*, 1987; *Murphy and Vincent*, 1998; *Hibbins et al.*, 2007; *Hoffmann et al.*, 2010], the MU radar [*Tsuda et al.*, 1990; *Nakamura et al.*, 1993], MST radars, [*Hitchman et al.*, 1991; *Fritts et al.*, 1992], VHF radars [*Fritts and Yuan*, 1989; *Wang and Fritts*, 1990], Rayleigh lidars [*Senft and Gardner*, 1991; *Collins et al.*, 1997; *Gardner and Liu*, 2007] and airglow imaging [*Swenson et al.*, 1999; *Espy et al.*, 2004]. These studies have addressed the seasonal variations of GWs, particularly, the one noted feature of GW climatologies common to these observations, namely, the semiannual variation in the GW activity at mesospheric heights with maximum activity occurring during the winter and summer months.

[1]School of Physics and Chemistry, University of Adelaide, Adelaide, South Australia, Australia.
[2]Research Institute for Sustainable Humanosphere, Kyoto University, Kyoto, Japan.
[3]Equatorial Geophysical Research Laboratory, Indian Institute of Geomagnetism, Tirunelveli, India.

0148-0227/11/2011JD015625

[4] Most of the GW observations described above have been made at midlatitudes to high latitudes. There is a lack of information on gravity waves in the equatorial region, where observations have been limited to only a few locations. Even where long sequences of mesospheric wind observations have been made earlier, such as at Tirunelveli and Jakarta, the emphasis has been on studies of prevailing winds, tides and long-period waves [*Gurubaran and Rajaram*, 1999; *Tsuda et al.*, 2002]. Only at Hawaii (22°N, 157°W) have comprehensive GW measurements been made in the mesosphere [*Isler and Fritts*, 1996; *Connor and Avery*, 1996; *Gavrilov et al.*, 2003], although some limited observations were reported for the lower-latitude site of Jicamarca [*Fritts et al.*, 1992, 1997; *Riggin et al.*, 1997a]. More recently, intensive studies of GW motions have commenced in the equatorial region using MF [*Gavrilov et al.*, 2004; *Kovalam et al.*, 2006; *Sridharan and Satish Kumar*, 2008] and meteor radars [*Antonita et al.*, 2008; *Clemesha et al.*, 2009; *Vincent et al.*, 2010]. These studies have reported the gravity wave variability on time scales ranging from diurnal through seasonal to intraseasonal and interannual.

[5] Theoretical studies of GWs have likewise made significant advances in the past decade. Numerical simulations and theoretical studies have addressed the excitation and effects of GWs and their role in providing a mean forcing on the middle atmosphere [*Fovell et al.*, 1992; *Alexander et al.*, 1995; *Horinouchi et al.*, 2002; *Kawashima*, 2003]. Convection is believed to be the main wave source in the tropics. In particular, short-period GWs excited by convection have the potential to influence up to very high altitudes in the mesosphere because they often have large vertical wavelengths and horizontal phase speeds that enable them to more readily escape critical level absorption [e.g., *Andrews et al.*, 1987; *Holton*, 1992]. They may play an important role in forcing the MSAO [*Burrage et al.*, 1996]. The forcing of waves with large vertical wavelengths and phase speeds is favored by deep convection [*Salby and Garcia*, 1987], and the most energetic waves are excited by the most intense convection having largest vertical motions [*Piani et al.*, 2000; *Lane et al.*, 2001]. The combination of these influences makes the equatorial convective zones the dominant source regions for high-frequency GWs.

[6] Our objectives in this paper are to (1) study the variability of GWs at small temporal scales using the data collected with low-latitude MF radars and (2) examine their relationship with the wave sources in the lower atmosphere. As convection is believed to be the main wave source in the tropics, the radars located in the vicinity of subtropical and tropical deep convective regions are ideal for examining the changes in the mesosphere due to this source. The studies are motivated by the works of *Alexander et al.* [2000] and *Alexander et al.* [2008] who analyzed the impact of convectively generated waves on the tropical middle atmosphere. *Alexander et al.* [2000] used NASA's ER-2 aircraft wind observations and *Alexander et al.* [2008] used EAR wind measurements and satellite (OLR/TRMM) data to examine the relationship between the stratospheric gravity waves and the deep convective clouds.

[7] MF radar observations used in this study were made at Tirunelveli, India (8.7°N, 78°E) and Pameungpeuk, Indonesia (7.5°N, 107.5°E), between February and March 2010. The paper is organized as follows. In section 2 we discuss the data analysis techniques. The analyzed results are presented in section 3. In section 4 we discuss the results and finally a summary of findings is presented in section 5.

2. Data Collection and Analysis

2.1. MF Radar

[8] MLT wind data acquired by spaced antenna MF radars located at Tirunelveli and Pameungpeuk for the period February-March 2010 are used to study the variability of short-period (20–120 min) gravity waves in the MLT region. The Pameungpeuk and Tirunelveli MF radars operate at 2 and 1.98 MHz, respectively. Observations are made over the altitude range 60–98 km with wind measurements made at 2 km height intervals at every 2 min. The lack of ionization at night restricts the useful data above ~78 km. Further operational details of the radars can be found in the work of *Briggs* [1984] and *Vincent and Lesicar* [1991]. MF radar mean winds at Tirunelveli have been reported earlier [*Rajaram and Gurubaran*, 1998]. In other studies, long-term observations from Pameungpeuk and Kototabang (0.2°S, 100.3°E) have been used to examine the longitudinal variability of long-period waves [*Sridharan et al.*, 2006] and terdiurnal tide [*Venkateswara Rao et al.*, 2011] in the MLT region.

[9] Since the MF radar located at Tirunelveli is situated near the dip equator (0.18°N), the radar derived motions above 94 km often reflect the drift velocity of the irregularities immersed in the bottom portion of the equatorial electrojet (EEJ) [*Gurubaran and Rajaram*, 2000], an intense east-west current flowing in an altitude region centered at ~105 km over the magnetic dip equator. At these times, the radar velocities above 94 km need not represent the neutral winds. Therefore, in these studies we have used horizontal wind measurements between 86–92 km altitudes for computing gravity wave fluxes, where the EEJ effects are expected to be negligible.

[10] Not all 2 min measurements at a given height produced reliable wind measurements due to the lack of suitable back scattering irregularities. To help overcome this limitation, data for each wind component were averaged in 10 min sample bins. Short gaps in the 10 min time series were linearly interpolated. Time series of 10 min samples of u (zonal) and v (meridional) were then organized in 1 day blocks and harmonically analyzed to find the prevailing wind and 24 and 12 h tidal components which were then subtracted from the data. This process gave time series of u', v' perturbations which were then broken into 4 h segments so that the mean square amplitudes in the period range 20 min to 4 h could be computed using power-spectral methods. Those segments for which either the tidal fit was poor and/or where there were less than 50% data points present were not used in the further analysis. A noise floor was calculated and subtracted from the spectra at each height in order to correct for the effects of external noise and measurement errors [*Press et al.*, 1992]. Finally, the GW variances ($\overline{u'^2}$, $\overline{v'^2}$) for the 20–120 min period range were computed by integrating the power spectral density in the period range between 20 and 120 min.

2.2. Satellite Data Sets

[11] To explore the relationship between the deep tropical convection and gravity wave variability observed at MLT

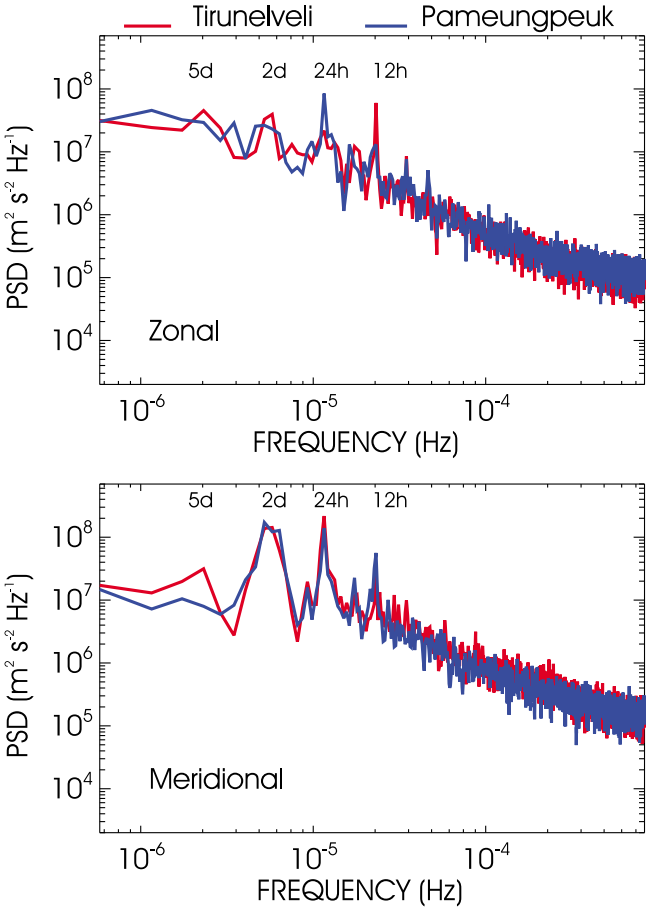

Figure 1. Frequency spectra of 10 min averaged (top) zonal and (bottom) meridional winds averaged between 86 and 92 km at (red line) Tirunelveli and (blue line) Pameungpeuk for the period between February and March 2010.

heights, we need information on lower-atmospheric sources that generate GWs. As the generation of atmospheric waves in the troposphere is related to convective activity, OLR (outgoing long-wave radiation)/cloud top temperature has been used in many studies [*Wheeler and Kildas*, 1999; *Miyoshi and Fujiwara*, 2009] as an index of wave excitation intensity. To examine the relationship between GW intensities and convective activity, we use two types of data sets, namely, (1) daily OLR which is available at 2.5° × 2.5° grid from National Oceanic and Atmospheric Administration (NOAA) satellite data and (2) rain rates available from the Tropical Rainfall Measuring Mission (TRMM) satellite data archive. The Tropical Rainfall Measuring Mission (TRMM) is a joint United States Japan satellite mission and provides crucial measurements such as the 2 km rainfall and storm height (the maximum height at which precipitation echoes are observed) in the tropical and subtropical regions. The daily rain rates which are available at 2.5° × 2.5° grid from 3B42 version 6 data product from the precipitation radar are used in this study.

3. Results

3.1. Frequency Spectra

[12] We begin by showing the frequency spectra of wind velocity for the time interval from February to March 2010 observed with Tirunelveli and Pameungpeuk MF radars. Figure 1 shows the mean spectra of the zonal and meridional winds derived from the two months of simultaneous data obtained at Pameungpeuk and Tirunelveli. The spectrum for each wind component was constructed by subdividing the data into 20 day intervals and averaging the power spectra computed for each interval. The segments were overlapped by 50% in order to minimize the variance associated with each spectral estimate [*Press et al.*, 1992]. Spectra computed for four heights from 86 to 92 km were averaged together to further improve the spectral reliability. Prominent spectral peaks associated with the diurnal (24 h), semidiurnal (12 h) and terdiurnal (8 h) tides are clearly evident in Figure 1. The semidiurnal tide dominates over the diurnal tide at Tirunelveli (red curve) in the zonal component. In contrast, at Pameungpeuk (blue curve) the diurnal tide is dominant in both wind components. Also, the diurnal tidal amplitudes are larger at Pameungpeuk than at Tirunelveli, only in the zonal component. Conversely, the semidiurnal amplitudes in the zonal component observed at Tirunelveli are approximately three times larger than those at Pameungpeuk. At periods longer than 1 day, however, energy is less equally distributed. The broad peak with a period near 2 days in the meridional component is due to the quasi-2-day wave, which is a strong feature of the mid latitude summer mesosphere, particularly, in the Southern Hemisphere [*Salby*, 1981; *Salby et al.*, 1984; *Harris*, 1994]. Longer-period variations in the zonal wind have larger amplitudes, partly due to much larger seasonal changes in this component.

[13] At periods shorter than a day, the spectral densities decrease with an approximate $f^{-5/3}$ power law. This part of the spectrum is ascribed to high-frequency gravity wave motions [see, e.g., *Fritts and Isler*, 1994, and references therein].

[14] The frequency spectra of winds observed with Tirunelveli and Pameungpeuk MF radars show slopes of ~−5/3 in the frequency range from 4×10^{-5} Hz to 3×10^{-4} Hz, but at frequencies $>3 \times 10^{-4}$ they are enhanced due to the effects of external noise and measurement errors [*Hines*, 1991; *Rastogi et al.*, 1996]. A noise floor was calculated for frequencies greater than 3×10^{-4} Hz and uncertainties in the estimated total variances were ~40 $m^2 s^{-2}$.

3.2. Gravity Wave Variance Studies

[15] The power spectra shown in Figure 1 reveal motions occurring over a wide range of frequencies with distinct peaks at tidal and 2 day wave periods, and continuum of gravity waves with periods ranging from the 20 min Nyquist up to the tidal periods and beyond. Small-scale GWs with periods of <1 h have been shown to be responsible for as much as 70% of the wave-induced transport that occurs in the MLT region [*Fritts and Vincent*, 1987]. In order to investigate the temporal variability of wave fluxes, daily values of wave variances for periods in the 20–120 min range were computed. Time series of daily values of $\overline{u'^2}$ (red curve) and $\overline{v'^2}$ (blue curve) at Tirunelveli are shown in Figure 2 for altitudes of 86, 88, 90 and 92 km. Successive heights are displaced by 400 $m^2 s^{-2}$. As can be seen, the GW variances show significant day-to-day variability with temporal modulations in the period range ~2–10 days. Both zonal and meridional components tend to show increase in amplitude with increasing height (z) almost at all times,

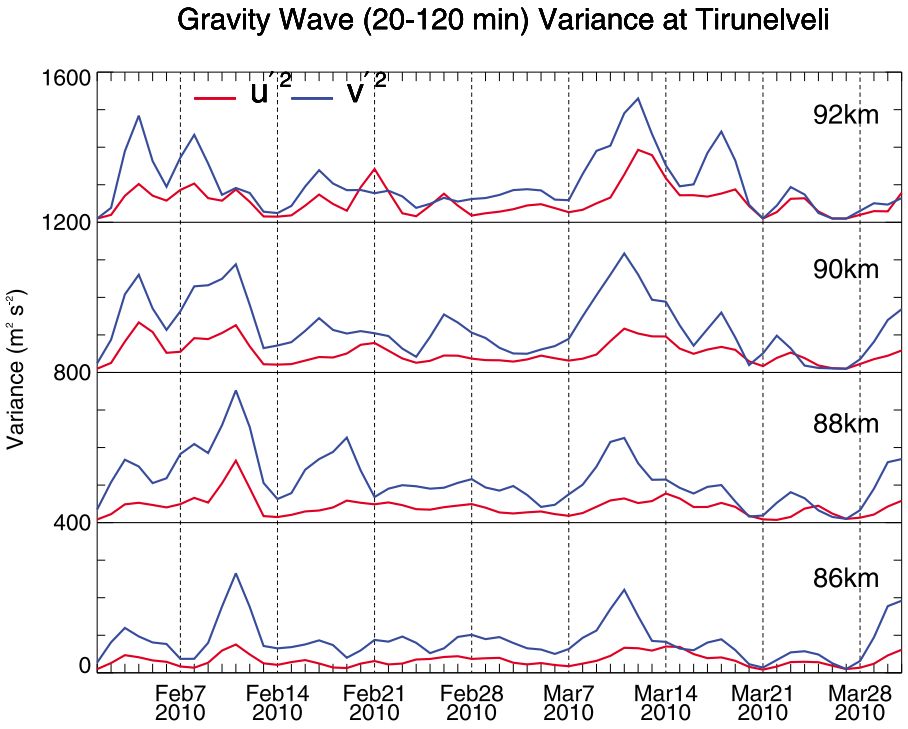

Figure 2. Daily variations of (red) zonal and (blue) meridional GW variance (20–120 min) at Tirunelveli at heights of 86, 88, 90, and 92 km during the period February to March 2010. Successive curves are displaced by 400 m^2 s^{-2}.

although at a slower rate than the $e^{z/2H}$ growth required to compensate for the decreasing density (here, H is the scale height). Between 2–7 February and 7–14 March, for example, GW variances are observed to increase with altitude. This is consistent with earlier radar observations [*Vincent and Fritts*, 1987; *Tsuda et al.*, 1989; *Isler and Fritts*, 1996] and model spectra [*Smith et al.*, 1987], which attribute the slower growth of motions occurring at larger vertical scales to the saturation of motions at smaller scales.

[16] It is evident from Figure 2 that the variances between 86–90 km, in particular, the meridional component at Tirunelveli show large enhancements during two intervals of the observational period. The first interval spans from 3 to 14 February, and the second interval spans from 5 to 21 March. During this period, enhancements appear in both the zonal and meridional wind components of the GW variances, but are stronger in the meridional component, with values reaching as high as ~350 m^2 s^{-2}. This preference for enhanced variances in meridional component was also noted in the earlier MF radar wind observations [*Vincent and Fritts*, 1987; *Isler and Fritts*, 1996]. In comparison with meridional variances, relatively little enhancements are observed in the zonal component. The variability in the $\overline{u'^2}$ and $\overline{v'^2}$ was found to be greatest in February and possibly associated with the quasi-2-day wave (see section 3.4) that was prominent around that time.

[17] Similar time series of daily GW variances for Pameungpeuk are plotted in Figure 3. As noted at Tirunelveli, the GW variances at Pameungpeuk also exhibit significant fluctuations in time scales in the range 3–7 days, and also the variances show steady growth with increasing height. Meridional variances reach largest values (88–90 km) just after mid-February, while zonal variances show enhancements after first week of March. Zonal variances are dominated by transient wave activity in 0.15–0.3 cpd (cycles per day), which are in agreement with the gravity wave observations reported earlier over the equatorial Pacific [*Riggin et al.*, 1997b; *Kovalam et al.*, 1999; *Tsuda et al.*, 2002]. Periodicity of ~7 days above 86 km are also observed during 7–14 March. In contrast to Tirunelveli, the amplitude of GW variances are smaller at Pameungpeuk.

[18] The strong short-term variations in wave activity seen in Figures 2 and 3 may be due to number of reasons. The primary source region for mesospheric waves is thought to be troposphere. Thus part of the variability may be caused by the short-term modulations of source strengths. Indeed, previous observations have shown gravity wave activity to be closely correlated with source modulations [*Nastrom and Eaton*, 1995; *Sato and Fukao*, 1995]. This aspect is later explored in section 4. Also, critical layer interactions due to changing background winds are expected to modulate or selectively filter the gravity waves as they propagate up through the middle atmosphere. Such process are certainly important here because of the large amplitudes and variability of the lower-frequency winds (e.g., diurnal tide, 2 day wave). Diurnal tides themselves interact with gravity waves and will modify the GW fluxes [*Fritts and Vincent*, 1987], a topic discussed further in section 3.4. It is noteworthy that at both Tirunelveli and Pameungpeuk, meridional amplitudes ($\overline{v'^2}$) are generally larger than zonal ($\overline{u'^2}$) which suggest a significant anisotropy in the horizontal distribution of the wave energy. Anisotropy is another feature which is not uncommon in middle atmosphere wave studies [*Vincent and Fritts*, 1987].

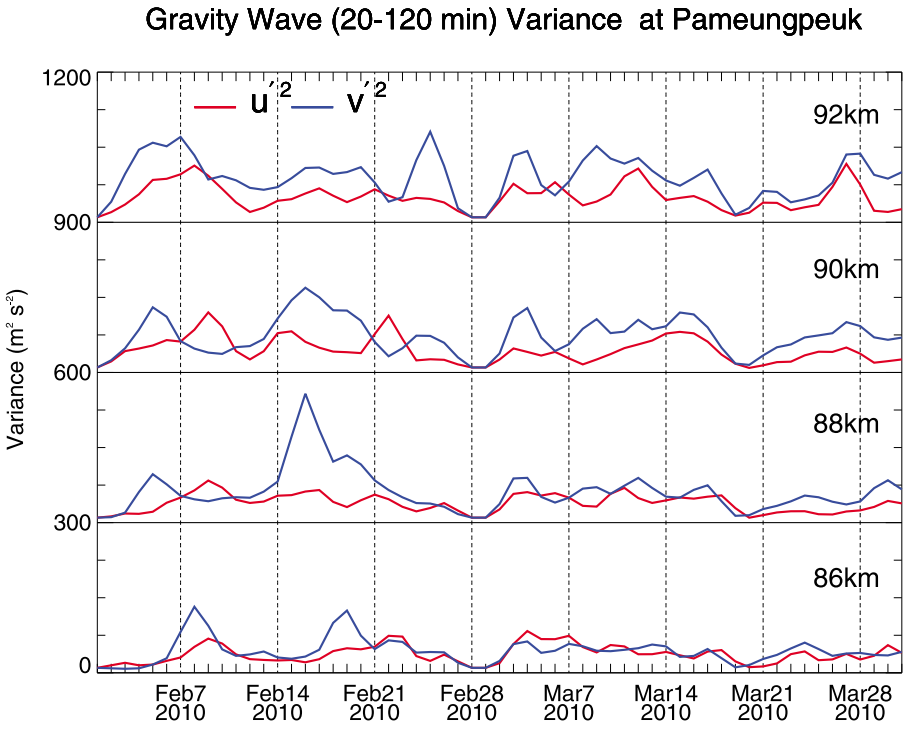

Figure 3. As for Figure 2 but for Pameungpeuk. Successive curves are displaced by 300 m^2 s^{-2}.

[19] The 2 month averages of the variance of the northward wind component ($\overline{v'^2}$) in the 86–92 km height range over Tirunelveli and Pameungpeuk were estimated to be 105 and 67.5 m^2 s^{-2}, respectively, whereas the 2 month averages of the variance of the eastward wind component ($\overline{u'^2}$) were 46.5 and 42.7 m^2 s^{-2}, respectively. The difference in the variance between eastward and northward components is considered to be due to the anisotropy in the horizontal propagation direction of GWs which is discussed further in section 3.3. In the 86–92 km height range, the 2 month averages of the total mean square amplitude, $\overline{u'^2}+\overline{v'^2}$, of the wind fluctuations with periods between 20 and 120 min observed with Tirunelveli and Pameungpeuk MF radars are about 152 and 110 m^2 s^{-2}, respectively. It is interesting to note that there is little difference between the GW amplitudes observed at Tirunelveli and Pameungpeuk located at 8° north and south of the equator, respectively. Some confirmation for this viewpoint comes from studies made at midlatitudes [*Tsuda et al.*, 1994a; *Nakamura et al.*, 1993]. Using the MU radar in Shigaraki and MF radar at Buckland Park in Adelaide, Australia, *Nakamura et al.* [1993] made comparisons between Kyoto (35°N) and Adelaide (35°S), located at conjugate points relative to the equator, and found that the GW energy in the mesosphere over those regions was fairly similar.

3.3. Propagation Direction

[20] A comparison of meridional and zonal wave variances, illustrated in Figures 2 and 3, shows that $\overline{v'^2}$ tends to be larger in magnitude than $\overline{u'^2}$. Between 86–92 km altitude region, the monthly mean $\overline{v'^2}/\overline{u'^2}$ variance ratio at Pameungpeuk is greater than 1.5. In the case of Tirunelveli observations the ratio is greater than 2. Using the MF radar wind data from Buckland Park MF radar (35°S), *Vincent and Fritts* [1987] observed the ratios ($\overline{v'^2}/\overline{u'^2}$) predominantly larger than unity for the gravity waves in the 60 min to 8 h band. This tendency is also seen in the observed ratios at Tirunelveli and Pameungpeuk. These observations suggest that the wave field is partially polarized with wave motions aligned more in the north-south direction than in the east-west direction.

[21] One method of examining the wave directionality is by measuring the bulk wave polarization of the band of waves contained in the finite time series. A measure of the polarization associated with quasi-monochromatic waves is easily derivable by using the so called Stokes parameter method described by *Vincent and Fritts* [1987]. Stokes' method makes use of the wave intensities and permits the calculation of the degree of polarization of the observed gravity wave band motions and the azimuthal orientation of this polarization. Stokes' parameters were determined using 5 day means of 20–120 min variances of zonal ($\overline{u'^2}$) and meridional ($\overline{v'^2}$) motions and their covariance $\overline{u'v'}$.

[22] Dominant directions of horizontal propagation were determined for the entire observational period over the 86–92 km altitude range. In order to obtain a measure of the dominant direction of horizontal propagation, the directions were binned into 30° angular segments and then the energy weighted average angular spectrum Φ_i was formed, so that for the ith segment

$$\Phi_i = \frac{\sum E_j}{E_{tot}} \tag{1}$$

$$\text{Here} \qquad E_j = \overline{u'^2} + \overline{v'^2} \tag{2}$$

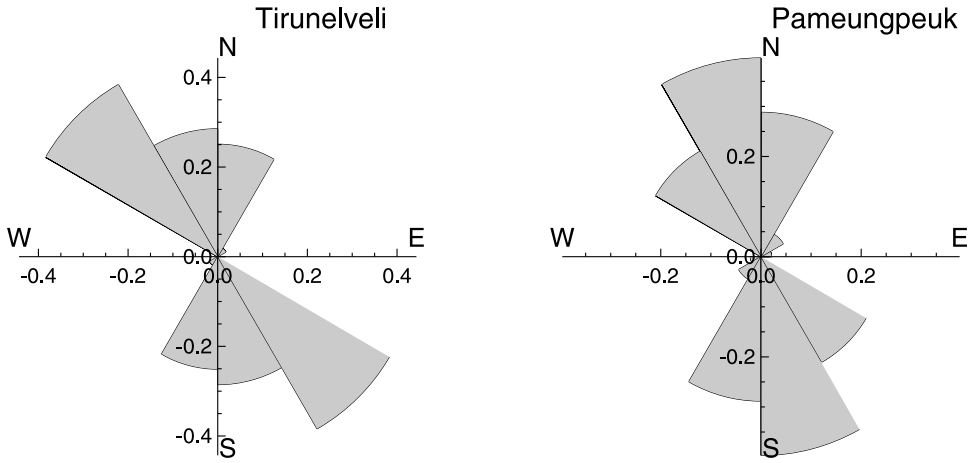

Figure 4. Angular distribution of dominant directions of horizontal propagation at (left) Tirunelveli and (right) Pameungpeuk for the period February-March 2010 and between 86 to 92 km.

represents the wave energy of GWs with periods between 20 and 120 minutes and the summation is taken over the j number of waves detected in the ith 30° angular segment. E_{tot} represents the total energy for the entire 2 month observational period over the 86–92 km altitude range. Histograms of Φ for Tirunelveli and Pameungpeuk are plotted in Figure 4. These plots can be taken to represent the "angular spectra" of wave energy for all data in the 86–92 km height range. Note that the polarization orientation shown in Figure 4 are subject to 180° ambiguity, and for presentation purposes have been reflected so that the points that differ from 180° represent the same information. As is evident from Figure 4, the waves tend to be polarized in the NW/SE direction over Tirunelveli (left panel). At Pameungpeuk, the total wave field exhibits a strong preference for SSE/NNW propagation. It is important to mention here that the actual direction of wave propagation was not computed as we have not used the vertical velocity data in this work and, hence direct comparison of the polarization orientation obtained at Tirunelveli and Pameungpeuk cannot be made. However, these results suggest that a significant degree of directional anisotropy can exist in the MLT region, a result which has implications for the initializations of the various parameterization schemes. Although the actual direction of wave propagation is unknown it is apparent that the angular distributions at both the locations have a strong meridional bias. This preference for a meridional direction of wave propagation at midlatitudes in the Southern Hemisphere middle atmosphere was reported by *Vincent and Fritts* [1987] and *Eckermann and Vincent* [1989] using MF radar data from Buckland Park, Australia. However, wave propagation at midlatitudes in the Northern Hemisphere exhibited more east-west alignment [*Nakamura et al.*, 1993].

3.4. Gravity Wave Variances and Tides

[23] Time series of $\overline{u'^2}$ and $\overline{v'^2}$ observed in the 86–92 km height region and made with a time resolution of 1 day show significant day-to-day variability in wave activity. Day-to-day fluctuations in the gravity wave variances were also noted by *Vincent and Fritts* [1987] who attributed this feature to the time variation in the source regions and to the filtering effects of the strong zonal winds in the middle atmosphere.

[24] Observations of short-period gravity wave modulation by tidal winds have also been reported earlier by *Fritts and Vincent* [1987], *Thayaparan et al.* [1995], and *Connor and Avery* [1996]. In order to understand the GW amplitude modulation by the background winds, we examine the time series of 2 h window calculations of GW variances (20–120 min) and 2-hourly averaged winds.

[25] Two examples for Tirunelveli data are presented in Figures 5 and 6 wherein, 2-hourly GW variances and high-pass mean winds (<10 days) for both zonal and meridional directions at 88 km are plotted. Note, that data with small gaps were excluded from the analysis. While these time series demonstrate considerable variability there is a noticeable tendency for the gravity wave variances to be largest when the tidal winds are strongest. As is evident in Figure 5, the peaks in GW variance are well correlated with the diurnal peaks (more westward). For example, peaks in GW variance occur on following days, 12 and 22 February and around 12 March. During these periods, the zonal winds attained westward speeds of ~30–50 m s^{-1}. Figure 6 shows the 2-hourly GW variances (top) and 2-hourly averaged meridional wind at 88 km. The 24 h tidal oscillation is clearly evident in the mean wind (bottom panel) as is the quasi-2-day wave particularly during 4–13 February.

[26] A noticeable feature in Figure 6 is the modulation of the GW variance at quasi-2-day period during 8–12 February. A 2 day wave can be seen in the 2-hourly averaged wind plot for the same interval. In response to this wave the GW variances are modulated at quasi-2-day periods as well. The 2 day modulation of GW variance was also noted by *Isler and Fritts* [1996] and *Herman et al.* [1999]. Also noticeable are the strong diurnal peaks in the GW variances and the northward winds for the periods during 14–21 February and 10–13 March.

[27] The time sequence of the 2-hourly GW variances and 2-hourly mean wind in the zonal and meridional directions at 88 km altitude over Pameungpeuk are presented in Figures 7 and 8, respectively. Large peaks in the zonal variance occur in groups of days and there are clear day-to-day modulations, e.g., 7–12 and 21–23 February and 7–14 March. It is apparent that large peaks in the variance are well correlated when the zonal wind had largest westward speeds. For example, large enhancements in the variance

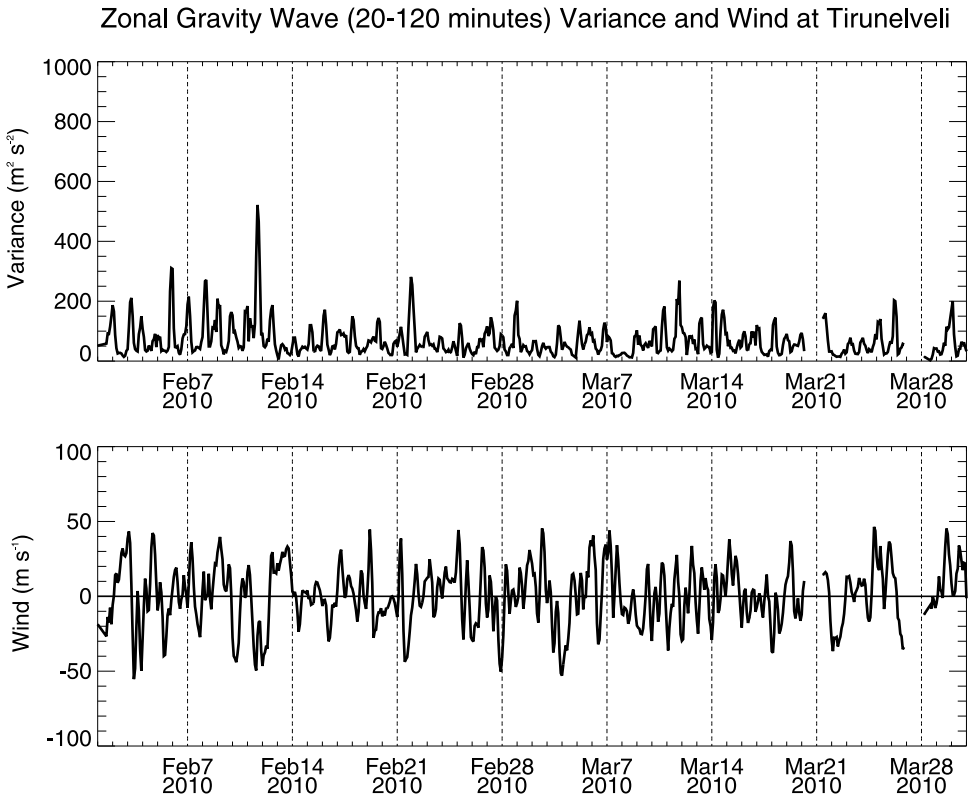

Figure 5. Time series of 2-hourly (top) zonal GW variances and (bottom) averaged winds at Tirunelveli for 88 km.

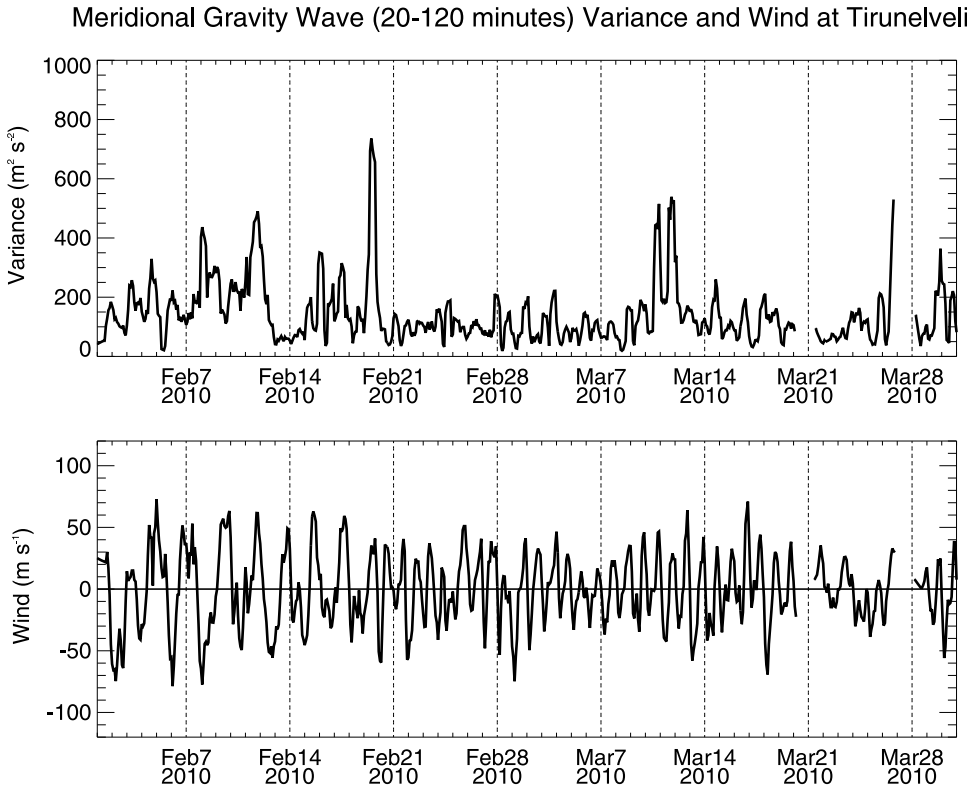

Figure 6. Same as Figure 5 but for meridional component.

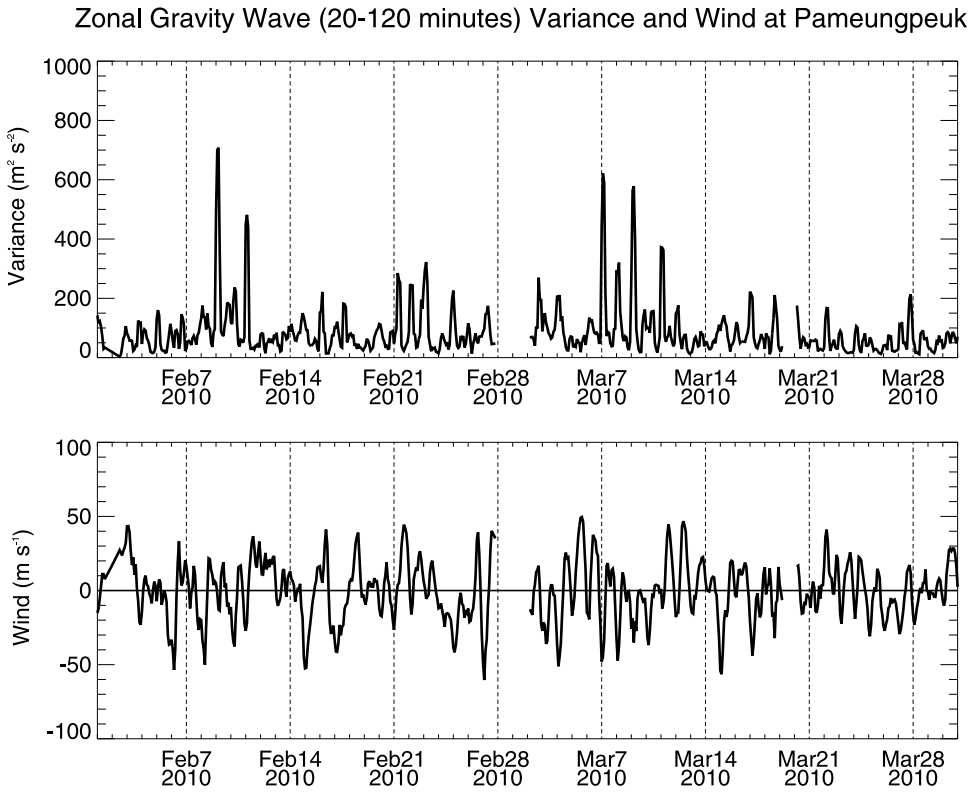

Figure 7. Time series of 2-hourly (top) zonal GW variances and (bottom) averaged winds at Pameungpeuk for 88 km.

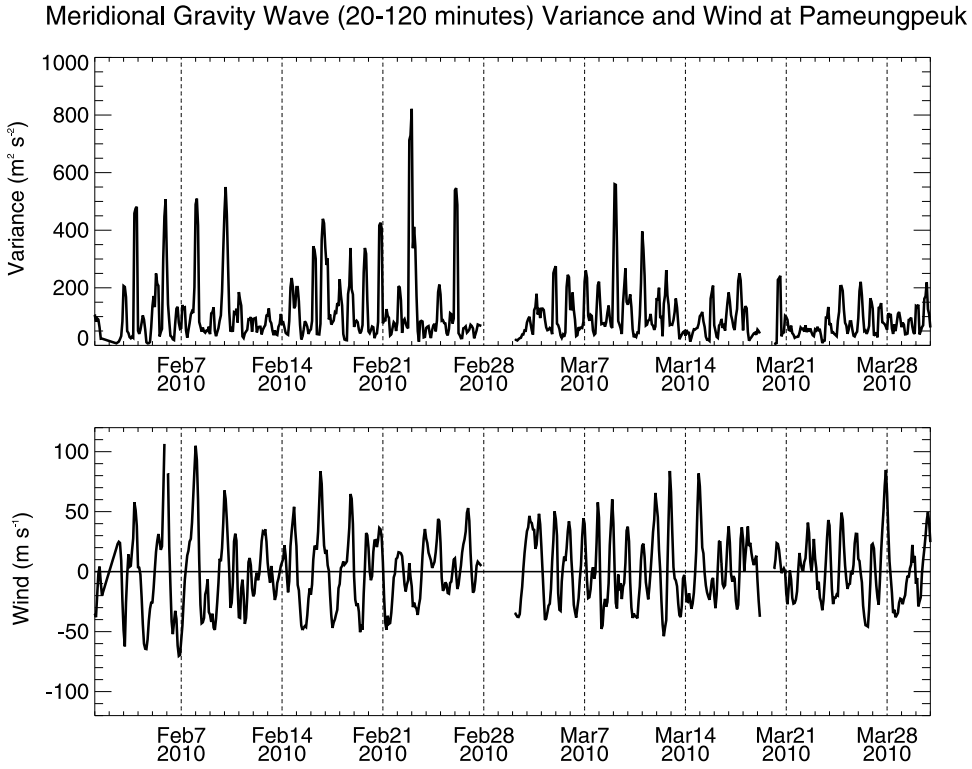

Figure 8. As for Figure 7 but for meridional component.

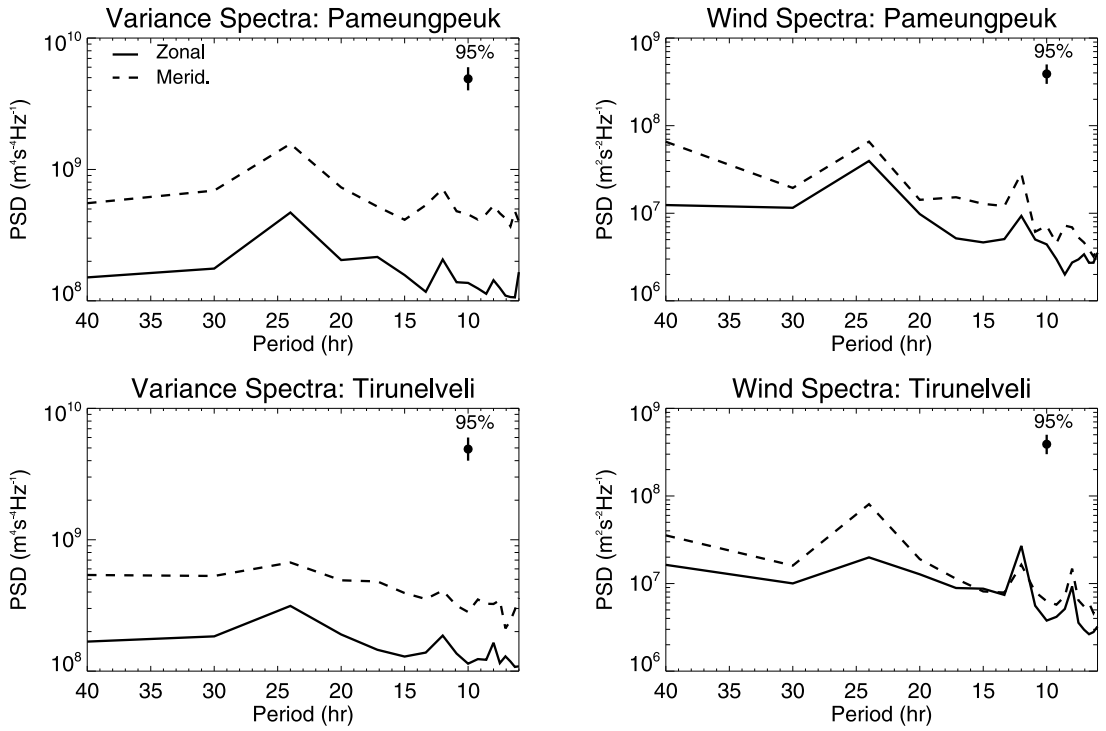

Figure 9. (top) Power spectra of the time series of 2-hourly (left) GW variances and (right) averaged winds between 86–92 km at Pameungpeuk for the period February-March 2010. Solid line indicates zonal component, and dashed line indicates meridional component. (bottom) Same as above but for Tirunelveli. Confidence limits at the 95% level are indicated.

seen on 17 February and 23 March occur during the intervals when the zonal wind has the westward amplitudes in the range 30–40 m s^{-1}. Large westward speeds exceeding 60 m s^{-1} are also observed in mid-March along with enhanced gravity wave activity. Figure 8 shows the 2-hourly GW variances (top) and 2-hourly averaged meridional wind (bottom) at 88 km. It is interesting to note here that GW variances show variability at quasi-2-day and tidal periods, e.g., 3–10 and 16–26 February and 7–14 March. At other heights (88–92 km), similar features were observed in the time series of GW variances and winds.

[28] For a more complete examination of the shorter-period variability of GW activity and its relationship with the background winds we have performed power spectral analysis of the time sequence of the 2-hourly GW variances and winds for the four heights taken over the entire 2 month period. The spectrum for each wind component was constructed by subdividing the time series in 5 day segments and averaging the power spectra computed for each segment. The segments were overlapped by 50% in order to minimize the variance associated with each spectral estimate. Spectra computed for four heights in the range 86–92 km were then averaged together to further improve the spectral reliability. At each height there were 23 overlapping segments giving a notional 23 × 2 × 9/11 ~37.6 degrees of freedom (*dof*). The factor of 9/11 arises from correlation between overlapping segments as can be found in the work of *Press et al.* [1992]. Averaging over 4 heights would increase the *dof* by a factor of 4, but it may be noted that the spectra from adjacent heights are not completely independent since the radar pulse length is about 4 km. It is conservatively estimated that there are about 75 *dof* associated with each spectral estimate. Figure 9 shows the spectra of time sequences of GW variance (left panel) and 2-hourly mean wind (right panel). Confidence limits at 95% level are shown.

[29] Strong peaks at 24 h are evident in the GW variances in zonal (solid) and meridional (dotted) directions at Pameungpeuk. Similarly, power spectra of wind (right panel) show peaks at 24 and 12 h periods. At Tirunelveli, zonal GW variance show enhancements at the 24 h period, while power spectra of zonal wind peaks at 24, 12, and 8 h periods. Interestingly, at both the locations power in the meridional component of GW variance and wind at the 24 h period is larger than the zonal component. At both locations, periods longer than 2 days dominate the power content of the signals. Otherwise, the diurnal component is the most dramatic feature of each spectrum. To a lesser extent, semidiurnal peaks are also evident.

[30] It is noteworthy that GW-tidal interaction is evident in the results presented here as reported earlier [see, e.g., *Fritts and Vincent*, 1987]. *Forbes et al.* [1991] have shown that tidal modulations of the winds in the mesosphere may act to modulate gravity wave propagation and thus induce apparent tidal oscillations in gravity wave variances. To investigate the GW modulation at tidal periods, we examine the degree of correlation between the spectral peaks observed in the GW variance and wind spectra. We compute cross-spectra using the zonal and meridional components of winds and GW variances at each location. Cross-spectra provide another way of exploring the interaction between the mean winds and the GW activity. Mean cross-spectra were computed in a similar

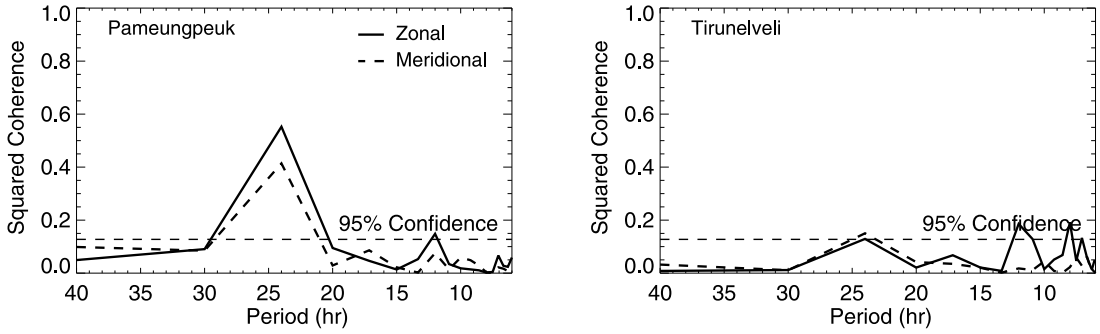

Figure 10. Squared coherence of 2-hourly GW variances and 2-hourly averaged winds at (left) Pameungpeuk and (right) Tirunelveli between 86–92 km for the period February-March 2010. Solid line indicates zonal component, and dashed line indicates meridional component. Confidence levels at the 95% are indicated by thin dashed line.

manner to the mean power spectra, that is in overlapping 5 day segments. The complex amplitudes were first averaged over all segments and then averaged over the four chosen heights before cross-spectral amplitudes were computed. The 2 month averaged cross-spectra between GW variance and wind spectra in terms of squared coherence are presented in Figure 10. The results for zonal(solid)/meridional(dashed) components are shown in Figure 10 for the period range 6–40 h.

[31] Considering first the zonal component for Pameungpeuk, we see that the coherence-squared values in zonal component are significant at 24 and 12 h periods. The 95% significant levels are indicated by a dashed line. The right panel in Figure 10 illustrates the squared coherence at Tirunelveli. A clear tendency for good correlation is also evident for the zonal component in this data. Squared coherence exhibit significant values at 24, 12, and 8 h periods. The meridional component (dotted line) in Figure 10 exhibits coherence squared values that are significant above the 95% significant levels. Large coherence squared values are seen at 12 and 8 h periods. The strong correlation between the gravity wave and diurnal tidal winds shown here are in accord with the many studies reported earlier [see, e.g., *Isler and Fritts*, 1996; *Nakamura et al.*, 1997; *Gurubaran and Rajaram*, 2001].

4. Discussion

[32] Horizontal wind observations from MF radars situated at Tirunelveli and Pameungpeuk were used to study GW motions in the 20 to 120 min band. We have examined ~60 days of MLT wind data between February and March 2010, during which both the stratospheric QBO and mesospheric SAO were in westward phase. Mean frequency spectra at both locations have revealed spectral peaks at tidal periods, broader peaks near ~2 days in the meridional component and enhanced GW activity at periods less than 24 h.

[33] Time series of $\overline{u'^2}$ and $\overline{v'^2}$ observed in the 86–92 km height region and made with a time resolution of 1 day show strong short-term variations in wave activity. The daily mean values of $\overline{u'^2} + \overline{v'^2}$ for Tirunelveli lie in the range 50–500 $m^2 s^{-2}$. Turning to the Pameungpeuk observations, the daily mean square values, $\overline{u'^2}$ and $\overline{v'^2}$, vary between ~50–300 $m^2 s^{-2}$ in the 86–92 km height range.

[34] These results can be compared with the other GW observational studies made at equatorial radar sites. *Vincent and Lesicar* [1991] used MF winds measured at Christmas Island to examine the dynamical state of the equatorial mesopause region during ALOHA-90. *Vincent and Lesicar* [1991] found daily values of variances in the range 50–200 $m^2 s^{-2}$ for GWs in 4 min to 1 h band at 86 km altitude. In their MF radar studies made at Hawaii, *Connor and Avery* [1996] and *Gavrilov et al.* [2004] have also reported values in the range 200–400 $m^2 s^{-2}$ for the 20 min to 4 h band for altitudes between 86 and 92 km. In an analysis of MF radar data taken from Christmas Island (2°N, 157°E), *Kovalam et al.* [2006] found that the total horizontal wind variance for February and March was about ~150–250 $m^2 s^{-2}$ for the 20–120 min band. In another GW study over equatorial site, Trivandrum, India, that involved analysis of meteor radar data taken between June 2006 and May 2007, *Antonita et al.* [2008] reported the total mean square amplitudes in the range 300–400 $m^2 s^{-2}$ between 86 and 92 km. Recently, in an analysis of data taken from Darwin VHF Meteor radar (12°S, 131°E), *Vincent et al.* [2010] retrieved high-frequency GW (<2 h) parameters using the wind observations acquired during the monsoon period (January-February 2010). They found that the mean square values varied between ~225 and ~600 $m^2 s^{-2}$. We compared the monthly mean values of GW variance in the range 50–300 $m^2 s^{-2}$ (Pameungpeuk) with the monthly mean GW variance from Darwin and found that they agree fairly well. Although, our results shown here are in good agreement with the MF/Meteor radar GW studies, we are unable to discern any clear seasonal trends in the wave activity due to relatively short amount of data. The observed differences in the GW wave variances between the two radar sites may represent latitudinal variability, though it is more probable that the differences occur due to the wave sources. A study made by *Miyoshi and Fujiwara* [2009] showed the longitudinal variation in GW energy in the equatorial thermosphere correlated with that of the convective activity in the tropical troposphere. We discuss this topic further in section 4.1.

[35] Time series of high-pass-filtered variances, $\overline{u'^2}$ and $\overline{v'^2}$, observed at 88 km show modulations at 12, 24, and 48 h periods. These results are in accord with *Forbes et al.* [1991] who have shown that tidal modulations of the winds in the mesosphere act to modulate gravity wave propagation,

and thus induce apparent tidal oscillations in gravity wave variances.

[36] Comparison of meridional and zonal wave variances illustrated in Figures 2 and 3 shows that $\overline{v'^2}$ tends to be larger in magnitude than $\overline{u'^2}$. The $\overline{v'^2}/\overline{u'^2}$ variance takes on values greater than unity, suggesting some degree of anisotropies in wave direction at Tirunelveli and Pameungpeuk. Plots of azimuthal distribution of wave energy shows that on an average, GWs over Tirunelveli were propagating in NW/SE quadrant, and at Pameungpeuk, the horizontal propagation of the polarized components were aligned in NNW/SSE quadrant. The anisotropy in the wave propagation direction noted here implies a strong contribution from meridionally propagating waves. This bias may be due to source effects and/or to the filtering effects of the zonal flow in the lower middle atmosphere. Thus GWs generated by tropospheric sources are strongly absorbed near the critical levels as they propagate toward the MLT regions. That is, interactions with the background wind field can modify the wave field by selective removal of waves which encounter critical levels, where their intrinsic wave speeds tend to zero.

[37] It is well known that the low-latitude site has unique seasonal zonal wind variations involving strong semiannual oscillation with the MSAO being out of phase with SAO. Observations reported in this work were made when SAO was in the eastward phase, so at this time GWs with prevailing eastward phase speeds propagating through the stratosphere are filtered out, and strong zonal anisotropy would be forced upon GWs reaching MLT heights. Since, the prevailing NS winds of the lower atmosphere are weak, GWs traveling northward or southward would propagate to the MLT with little anisotropy. Upon reaching MLT, the GWs become saturated and their amplitudes are limited to the intrinsic phase speed ($|u' - c|$) where u' is the background wind and c is phase speed of the wave. The background wind that vertically propagating waves encounter in the MLT are modified by the bulk flow (where the bulk flow is the sum of prevailing mean wind and tidal components). Gravity waves amplitude will then get modified by the bulk flow and develop modulations in east-west/north-south directions. It should be emphasized here that for the February–March data the latitudinal difference of the mesospheric winds is about 5 m s^{-1} and is not great enough to cause any preference in the directions illustrated in Figure 4.

[38] Meridional variances ($\overline{v'^2}$) are somewhat larger than zonal variances ($\overline{u'^2}$). The high degree of variability on time scales of ~7–10 days evident in Figures 2 and 3 (particularly in $\overline{v'^2}$), may be due to changing source and propagation direction since these time scales are also characteristics of strong convective systems over the Indonesian regions [*Tsuda et al.*, 1994b].

[39] Hence, another possibility for the observed meridional bias in the propagation direction is the powerful source region either to the north (south) of Pameungpeuk (Tirunelveli). In this regard, it is interesting that previous MLT observations of gravity waves have also indicated anisotropy in the wave propagation direction [*Sridharan and Satish Kumar*, 2008; *Nakamura et al.*, 2003]. *Sridharan and Satish Kumar* [2008] studied the seasonal variation of GW variances in 2–6 h period band at mesospheric heights over Tirunelveli. Using hodograph analysis of MF radar winds, they found the direction of wave motions in the NW/SE quadrant. It is noteworthy that the predominant propagation direction, namely, NW/SE, shown here is in agreement with the findings of *Sridharan and Satish Kumar* [2008]. Though the directions are determined with an ambiguity of 180°, considering the powerful source of wave generation south of India, the propagation direction would be from SE to NW, rather than from NW to SE. In another study, *Nakamura et al.* [2003] examined the OH airglow images obtained at Tanjunsagri, Indonesia (7°S, 109°E) and reported that gravity waves mainly propagated southward. The results reported here for Pameungpeuk also show a preference of SE/NW direction. Again considering the active convection to the North of Pameungpeuk, the propagation direction would be from NW to SE in accord with the results of *Nakamura et al.* [2003]. As the measurements reported here were made during the period when the convection was active in the Indonesian Maritime Continent region, the distribution of convective sources in the lower atmosphere could possibly produce the observed wave propagation direction in the mesosphere, a topic which is further discussed below.

4.1. Wave Sources

[40] The most interesting property of the both set of observations shown earlier (see section 3.3) is the relatively narrow range of azimuths within which these waves seem to preferentially propagate in a given season. This anisotropy in the wave propagation direction therefore cannot be due to critical layer filtering alone but must also be source related. Tropical convection is the most likely source for the gravity wave generation. The association of GWs with deep tropical convection has also been established by space-borne OLR observations [*Salby et al.*, 1991; *Bergman and Salby*, 1994].

[41] A prolific source of wave generation is the extensive region of deep convection over the Indonesian region during these months. Some observational confirmation for this viewpoint comes from recent studies made with VHF radars which show substantial temporal variations in wave activity in the troposphere. Using VHF radar measurements, *Vincent et al.* [2004] presented GW variability with period in the range of 8–180 min in the lower troposphere in the vicinity of intense deep convective storms over Tiwi Islands (11.4°S, 130.5°E) in Northern Australia, and attributed convectively generated GWs to be the cause for the enhancements in the wave energy. Furthermore, results from four years of continuous wind observations made with VHF radar at Gadanki (13.5°N, 79.2°E) [*Dutta et al.*, 2008] also suggest deep tropical convection to be the main source of short-period (<2 h) GW activity in the troposphere and lower stratosphere. More recently, *Tsuda et al.* [2009] found that the spatial and seasonal variations of potential energy, E_p, to be closely related with the convective wave generation in the tropics. They show an enhancement in the wave activity in the western Pacific and Indian ocean during DJF/MAM months. These observations clearly suggest a close coupling between the lower and upper atmosphere by gravity wave flux originating in the tropical convection zones. Following the above findings, we attempt to investigate the relationship between GW activity at MLT heights and the deep tropical convection during the February–March 2010 campaign in the section below.

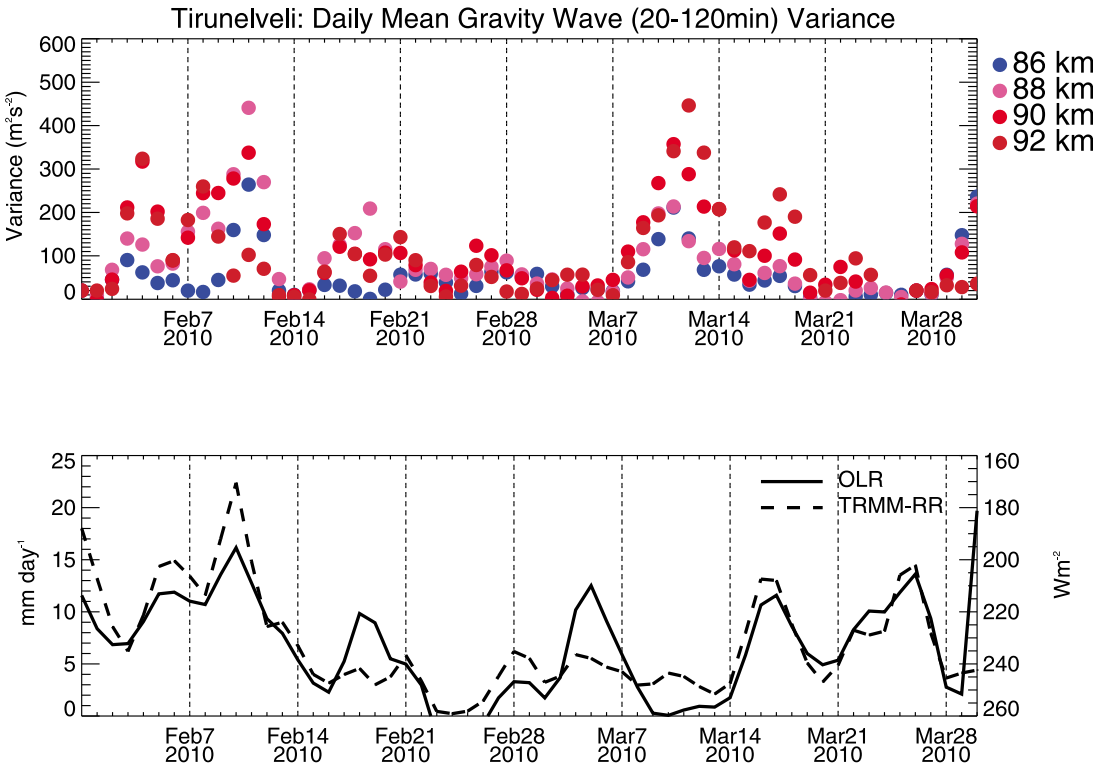

Figure 11. (top) Daily variation of GW variance at Tirunelveli between 86 and 92 km and for the period between February and March 2010. The colored circles represent the wave variances as a function of height for (blue) 86, (magenta) 88, (red) 90, and (brown) 92 km. (bottom) TRMM daily rain rate (dashed line, scale to the left) and OLR (solid line, inverted scale to the right). The daily OLR and TRMM rain rates (RR) were averaged over the longitude sector 80°E–100°E.

4.2. Correlation Between Gravity Wave Variance and Tropical Convection

[42] MF radar wind observations reported in this work were collected during February-March 2010 when the deep convection occurred over the maritime continent, the region including Indonesia and northern Australia. To examine further the relationship between gravity wave variance and the deep tropical convection, we employ a satellite data set of daily averaged OLR temperatures and TRMM rain rates (RR) as described earlier in section 2.2.

[43] In Figure 11 we show the daily variation of horizontal wind variances ($\overline{u'^2} + \overline{v'^2}$) (top panel) over 86–92 km altitude region along with the daily values of OLR and TRMM rain rates (bottom panel). Note that the OLR and TRMM fields were averaged over the longitude sector of 80–100°E and the latitude region 7°S–7°N anticipating that GW response to deep tropical convection would arise in this region. The scale for OLR brightness temperature is reversed in order to facilitate a visual comparison with temporal variations in GW activity. It is interesting to note in Figure 11 that largest values of wave variances occur above the coldest (high) clouds. Highest (coldest) cloud top temperatures of ~235 W m^{-2} have been used as a threshold in statistical studies of convection [*Chen et al.*, 1996] and global rainfall correlations [*Arkin and Meisner*, 1987]. Such deep convection is associated with heavy rainfall and deep regions of latent heating that can act as centers of GW forcing. This has been demonstrated in a mesoscale convection model [*Fovell et al.*, 1992; *Alexander et al.*, 1995; *Piani et al.*, 2000; *Lane et al.*, 2001]. In these simulations of a mesoscale convection model, the forcing of waves with large phase speeds and the most energetic waves are excited by the most intense convection having largest vertical motions. If the relationship in Figure 11 is representative of convection, then $\overline{u'^2} + \overline{v'^2}$ would show anticorrelation with OLR cloud top temperatures.

[44] There are several occasions when GW variances show enhancements at times of low OLR values. For example, enhancement in the GW variances (200–400 m^2 s^{-2}) occur at all heights around 7 and 12 February and 17 March, which are also the times when values of OLR range from 160–220 W m^{-2}. During the time when the OLR shows small values, TRMM rainfall rates show values in excess of 20 mm/day. For example, peaks in TRMM rain rates (bottom panel) observed on 7 February (14 mm/day), 11 February (22 mm/day) and 18 March (12 mm/day) coincide with low OLR values and confirm the presence of significant precipitation rates in latent heat release centered around these days. Strong enhancements in the GW activity at MLT heights suggest that high-frequency GWs were probably generated around these three periods when latent heat release over the longitude region 80–100°E was strongest.

[45] Figure 12 depicts the variations of GW variances, OLR and TRMM rain rates over Pameungpeuk similar to those shown for Tirunelveli in Figure 11. The daily OLR and

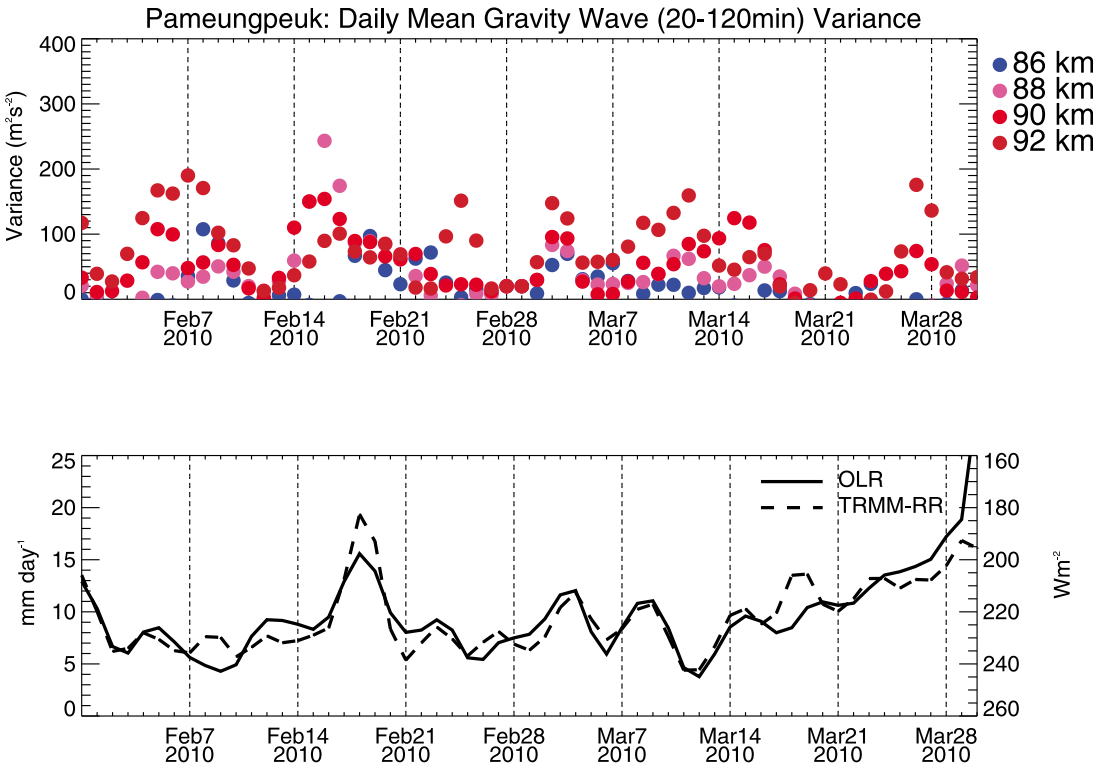

Figure 12. As for Figure 11 but for Pameungpeuk. The daily OLR and TRMM rain rates (RR) were averaged over the longitude sector 100°E–120°E.

TRMM fields were averaged over the longitude sector 100–120°E anticipating that GW response to deep tropical convection would arise in this region. Evident in Figure 12, top, is the 7–10 day modulation of gravity wave intensities occurring in four 10 day intervals. Daily OLR values shown in Figure 12, bottom, ranged from 180–220 W m^{-2}. It is interesting to note in Figure 12 that at times when the OLR values show small values, TRMM observations indicate significant rain rates. For example, enhancements of gravity wave intensity observed during 14–21 February are closely related with the low OLR value (~200 Wm^{-2}) and large rain rates (18 mm/day). Peaks in TRMM rain rates observed on 4 and 10 March (14 mm/day) coincide with low OLR values (~210 Wm^{-2}). One noticeable feature in Figure 11 is a gradual increase in the magnitude of gravity wave variances from 21 to 31 March, and this feature coincided with the decreasing/increasing values of OLR/TRMM rain rates. Overall, the strong variations of $\overline{u'^2}+\overline{v'^2}$ on time scale of 7–10 days and similar variations in daily OLR and TRMM rain rates suggest that source variability can be another potential contributor to the fluctuations in the GW variability.

[46] In this regard, it is interesting that recent high-resolution model studies of the equatorial thermosphere have found that the longitudinal variations in gravity wave energy due to short-period waves ~4 h in the stratosphere and mesosphere are similar, and closely related to the longitudinal location of the rainfall rate near the equator [*Miyoshi and Fujiwara*, 2009]. Other studies have demonstrated the dynamical coupling between the troposphere and the MLT region through the upward propagation of gravity waves [*Hocke and Tsuda*, 2001]. By using GPS-MET (meteorology) radio occultation, *Hocke and Tsuda* [2001] found that the longitudinal distribution of plasma irregularities in the MLT region were similar to that of the water vapor pressure in the tropics. Our observational results shown here agree with the above findings, and suggest that gravity waves generated by convection have the potential to have influences up to very high altitudes.

5. Summary

[47] In this study we have used MF radar wind observations from Tirunelveli and Pameungpeuk made between February and March 2010 in the investigation of temporal and spatial variability of short-period (20–120 min) gravity waves in the tropical MLT region. Time series of $\overline{u'^2}$ and $\overline{v'^2}$ observed between 86–92 km, and made with a resolution of 1 day show short-term variations in wave activity, particularly in the meridional component. The gravity wave activity at Tirunelveli and Pameungpeuk showed modulations in the scales of 3–7 days. Spectra of 2-hourly gravity wave variances exhibit a strong diurnal modulation and the gravity wave modulation at this period is an evidence for gravity wave/tidal interaction. Day-to-day variation of MLT gravity wave variances and its modulation over time scales of 7–10 days reported here appears to be due to the horizontal distribution of wave sources around the observational site. We also investigated the gravity wave activity in the MLT and their relation to lower-atmospheric wave variability. Our results indicate strong anticorrelation between OLR (cold temperature/low brightness temperature) and GW variance, suggesting a possible role of deep tropical convection in causing the gravity wave variability in the low-latitude MLT region. However,

confirmation, or otherwise of the above speculations can only come from improved and widely dispersed observations. The results provided here were obtained using too little data, and hence to assess either the role of other waves or their influence at greater heights, long-term observations will be necessary. Analysis of such data sets are under way, and will provide a more complete climatology of long-term gravity wave activity in future studies.

[48] **Acknowledgments.** The helpful comments of R.A. Vincent on early drafts of this paper are gratefully acknowledged. The Pameungpeuk MF radar is operated as a collaborative project between RISH and LAPAN. This study was supported by the Japanese Ministry of Education, Culture, Sports, Science and Technology (MEXT) through a Grant-in-Aid for Scientific Research (2253006). The first author would like to thank Research Institute of Sustainable Humanosphere (RISH) for the visiting professor's position offered to her and for providing facilities to carry out the present study.

References

Alexander, M. J., J. R. Holten, and D. Durran (1995), The gravity wave response above deep convection in squall line, *J. Atmos. Sci.*, *52*, 2212–2226.

Alexander, M. J., J. H. Beres, and P. Fister (2000), Tropical stratospheric gravity wave activity and relationships to clouds, *J. Geophys. Res.*, *105*, 22,299–22,309.

Alexander, S. P. T., T. Tsuda, Y. Shibagaki, and T. Kozu (2008), Seasonal gravity wave activity observed with the Equatorial Atmosphere Radar and its relation to rainfall information from the tropical rainfall measuring mission, *J. Geophys. Res.*, *113*, D02104, doi:10.1029/2007JD008777.

Andrews, D. G., J. R. Holton, and C. B. Leovy (1987), *Middle Atmosphere Dynamics*, Academic, Orlando, Fla.

Antonita, T. M., G. Ramkumar, K. K. Kumar, and V. Deepa (2008), Meteor wind radar observations of gravity wave momentum fluxes and their forcing toward the Mesospheric Semiannual Oscillation, *J. Geophys. Res.*, *113*, D10115, doi:10.1029/2007JD009089.

Arkin, P. A., and B. A. Meisner (1987), The relationship between large scale convective rainfall and cold cloud over Western Hemisphere during 1982–84, *Mon. Weather Rev.*, *115*, 51–74.

Baldwin, M. P., et al. (2001), The Quasi-Biennial Oscillation, *Rev. Geophys.*, *39*, 179–229.

Bergman, J. W., and M. L. Salby (1994), Equatorial wave activity derived from fluctuations in observed convection, *J. Atmos. Sci.*, *51*, 3791–3806.

Briggs, B. H. (1984), The analysis of spaced sensor records by correlation techniques, in *Handbook for the Middle Atmosphere Program*, vol. 13, pp. 166–186, Spec. Comm. for Sol.-Terr. Phys. Secretariat.

Burrage, M. D., R. A. Vincent, H. G. Mayr, W. R. Skinner, N. F. Arnold, and P. B. Hays (1996), Long-term variability in the equatorial mesosphere and lower thermosphere zonal wind, *J. Geophys. Res.*, *101*, 12,847–12,854.

Chen, S. S., R. A. Houze Jr., and B. E. Mapes (1996), Multiscale variability of deep convection in relation to large-scale circulation in TOGA COARE, *J. Atmos. Sci.*, *53*, 1380–1409.

Clemesha, B. R., P. Batista, R. A. B. da Costa, and N. Schuch (2009), Seasonal variations in gravity wave activity at three locations in Brazil, *Ann. Geophys.*, *27*, 1059–1065.

Collins, R. L., D. Thorsen, and S. J. Franke (1997), MF radar and Na lidar measurements of fluctuating winds in the mesopause region, *J. Geophys. Res.*, *102*, 16,583–16,591.

Connor, L. N., and S. K. Avery (1996), A three year gravity wave climatology of the mesosphere and lower thermosphere over Kauai, *J. Geophys. Res.*, *101*, 4065–4077.

Dunkerton, T. J. (1997), The role of gravity waves in the quasi-biennial-oscillations, *J. Geophys. Res.*, *102*, 26,053–26,076.

Dutta, G., T. Tsuda, P. V. Kumar, M. C. A. Kumar, S. P. Alexander, and T. Kozu (2008), Seasonal variation of short-period (<2 hr) gravity wave activity over Gadanki, India (13.5°N, 79.2°E), *J. Geophys. Res.*, *113*, D14103, doi:10.1029/2007JD009178.

Eckermann, S. D., and R. A. Vincent (1989), Falling sphere observations of anisotropic gravity wave motions in upper stratosphere over Australia, *Pure Appl. Geophys.*, *130*, 509–532.

Espy, P. J., G. Jones, G. R. Swenson, J. Tang, and M. J. Taylor (2004), Seasonal variation of the gravity wave momentum flux in the Antarctic mesosphere and lower thermosphere, *J. Geophys. Res.*, *109*, D23109, doi:10.1029/2003JD004446.

Forbes, J. M., J. Gu, and S. Miyahara (1991), On the interactions between the gravity waves and the propagating diurnal tide, *Planet. Space Sci.*, *39*, 1249–1257.

Fovell, R. G., D. Durran, and J. R. Holten (1992), Numerical simulations of convectively generated stratospheric gravity waves, *J. Atmos. Sci.*, *49*, 1427–1442.

Fritts, D. C., and M. J. Alexander (2003), Gravity wave dynamics and effects in the middle atmosphere, *Rev. Geophys.*, *41*(1), 1003, doi:10.1029/2001RG000106.

Fritts, D. C., and J. R. Isler (1994), Mean motions and tidal and two-day wave structure and variability in the mesosphere and lower thermosphere over Hawaii, *J. Atmos. Sci.*, *51*, 2145–2164.

Fritts, D. C., and R. A. Vincent (1987), Mesospheric momentum flux studies at Adelaide, Australia: Observations and a gravity wave-tidal interaction model, *J. Atmos. Sci.*, *44*, 605–619.

Fritts, D. C., and L. Yuan (1989), Measurement of the momentum fluxes near the summer mesopause at Poker Flat, Alaska, *J. Atmos. Sci.*, *46*, 2569–2579.

Fritts, D. C., L. Yuan, M. H. Hitchmann, L. Coy, E. Kudeki, and R. F. Woodman (1992), Dynamics of the equatorial mesosphere observed using Jicmarca MST radar during June and August 1987, *J. Atmos. Sci.*, *49*, 111–127.

Fritts, D. C., et al. (1997), Equatorial dynamics observed by rocket, radar, and satellite during the CADRE/MALTED campaign: 2. Mean and wave structures, coherence and variability, *J. Geophys. Res.*, *102*, 26,191–26,216.

Garcia, R. R., and F. Sassi (1999), Modulation of the mesospheric semiannual oscillation by the quasi-biennial oscillation, *Earth Planets Space*, *51*, 563–569.

Garcia, R. R., T. J. Dunkerton, R. S. Lieberman, and R. A. Vincent (1997), Climatology of the semiannual oscillation of the tropical middle atmosphere, *J. Geophys. Res.*, *106*, 26,019–26,032.

Gardner, C. S., and A. Z. Liu (2007), Seasonal variations of the vertical fluxes of heat and horizontal momentum in the mesopause region at Starfire Optical Range, *J. Geophys. Res.*, *112*, D09113, doi:10.1029/2005JD006179.

Gavrilov, N. M., D. M. Riggin, and D. C. Fritts (2003), Medium frequency radar studies of gravity wave seasonal variations over Hawaii (22°N, 60°W), *J. Geophys. Res.*, *108*(D20), 4655, doi:10.1029/2002JD003131.

Gavrilov, N. M., D. M. Riggin, and D. C. Fritts (2004), Interannual variations of the mean wind and gravity wave variances in the middle atmosphere over Hawaii, *J. Atmos. Sol. Terr. Phys.*, *66*, 637–645.

Gurubaran, S., and R. Rajaram (1999), Long term variability in the mesospheric tidal winds observed by MF radar over Tirunelveli (8.7°N, 78°E), *Geophys. Res. Lett.*, *27*, 943–946.

Gurubaran, S., and R. Rajaram (2000), Signatures of equatorial electrojet in the mesospheric partial reflection drifts over magnetic equator, *Geophys. Res. Lett.*, *27*, 943–946.

Gurubaran, S., and R. Rajaram (2001), Mean winds, tides and gravity waves during the westward phase of the mesopause semiannual oscillation (MSA0), *J. Geophys. Res.*, *106*, 31,817–31,824, doi:10.1029/2001JD000325.

Hamilton, K. P. (1982), Rocketsonde observations of the mesospheric semiannual oscillation at Kwajalian, *Atmos. Ocean*, *20*, 281–286.

Harris, T. J. (1994), A long-term study of the quasi-two-day wave in the middle atmosphere, *J. Atmos. Terr. Phys.*, *56*, 569–579.

Herman, R. L., W. A. Robinson, and S. J. Franke (1999), Observational evidence of quasi two-day/gravity wave interaction using MF radar, *Geophys. Res. Lett.*, *26*, 1141–1149.

Hibbins, R. E., P. J. Espy, M. J. Jarvis, D. M. Riggin, and D. C. Fritts (2007), A climatology of tides and gravity wave variance in the MLT above Rothera, Antarctica obtained by MF radar, *J. Atmos. Sol. Terr. Phys.*, *69*, 578–558.

Hines, C. O. (1991), The saturation of gravity waves in the middle atmosphere, II, Development of Doppler-spread theory, *J. Atmos. Sci.*, *48*, 1360–1379.

Hirota, I. (1978), Equatorial waves in the upper stratosphere and mesosphere in relation to the semiannual oscillation of the zonal wind, *J. Atmos. Sci.*, *35*, 714–722.

Hitchman, M. H., K. W. Bywaters, D. C. Fritts, L. Coy, E. Kudeki, and F. Suruchu (1991), Mean wind and momentum fluxes over Jicamaraca, Peru during June and August 1987, *J. Atmos. Sci.*, *49*, 2372–2383.

Hocke, K., and T. Tsuda (2001), Gravity waves and ionospheric irregularities over tropical convection zones observed by GPS/MET radio occultation, *Geophys. Res. Lett.*, *28*, 2815–2818.

Hoffmann, P., E. Becker, W. Singer, and M. Placke (2010), Seasonal variation of mesospheric waves at northern middle and high latitudes, *J. Atmos. Sol. Terr. Phys.*, *72*, 1068–1079.

Holton, J. R. (1992), *An Introduction to Dynamic Meteorology*, 3rd ed., Academic, San Diego, Calif.

Holton, J. R., and M. J. Alexander (1999), Gravity waves in the mesosphere generated by tropical convection, *Tellus*, *51*, 45–58.

Horinouchi, T., T. Nakamura, and J. Kosaka (2002), Convectively generated mesoscale gravity waves simulated throughout the middle atmosphere, *Geophys. Res. Lett.*, *29*(21), 2007, doi:10.1029/2002GL016069.

Isler, J. R., and D. C. Fritts (1996), Gravity wave variability and the interaction with the low frequency motions in the lower mesosphere and thermosphere over Hawaii, *J. Atmos. Sci.*, *53*, 37–38.

Kawashima, M. (2003), The role of gravity waves in the meso-β-scale cycle of squall-line type convective systems, *J. Meteorol. Soc. Jpn.*, *81*, 713–746.

Kovalam, S., R. A. Vincent, I. M. Reid, T. Tsuda, T. Nakamura, K. Ohnishi, A. Nuryanto, and H. Wiryosumarto (1999), Longitudinal variations in planetary wave activity in the equatorial mesosphere, *Earth Planets Space*, *51*, 665–674.

Kovalam, S., R. A. Vincent, and P. Love (2006), Gravity waves in the equatorial MLT region, *J. Atmos. Sol. Terr. Phys.*, *68*, 266–282.

Lane, T. P., M. J. Reeder, and T. L. Clark (2001), Numerical modeling of gravity wave propagation by deep tropical convection, *J. Atmos. Sci.*, *58*, 1249–1274.

Miyoshi, Y., and H. Fujiwara (2009), Gravity waves in the equatorial thermosphere and their relation to lower atmospheric variability, *Earth Planets Space*, *61*, 471–478.

Murphy, D. J., and R. A. Vincent (1998), Mesospheric momentum fluxes over Adelaide during the 2-day wave: Results and intrepretation, *J. Geophys. Res.*, *103*, 28,627–28,636.

Nakamura, T., T. Tsuda, S. Fukao, and S. Kato (1993), Comparison of the mesospheric gravity waves observed with the MU radar (35°N) and the Adelaide MF radar (35°S), *Geophys. Res. Lett.*, *20*, 803–806.

Nakamura, T., D. C. Fritts, J. R. Isler, T. Tsuda, R. A. Vincent, and I. M. Reid (1997), Short-period fluctuations of the diurnal tide observed with the low-latitude MF and meteor radars during CADRE: Evidence for gravity wave/tidal interactions, *J. Geophys. Res.*, *102*, 26,225–26,238.

Nakamura, T., T. Ano, and T. Tsuda (2003), Mesospheric gravity waves over a tropical convective region observed by OH airglow imaging in Indonesia, *Geophys. Res. Lett.*, *30*(17), 1882, doi:10.1029/2003GL017619.

Nastrom, G. D., and F. D. Eaton (1995), Variations of winds and turbulence seen by 50-MHz radar at White S ands Missile Range, New Mexico, *J. Appl. Meteorol.*, *34*, 2135–2148.

Piani, C., D. Durran, M. J. Alexander, and J. R. Holten (2000), A numerical study of three-dimensional gravity waves triggered by deep trpoical convection and their role in the dynamics of the QBO, *J. Atmos. Sci.*, *57*, 3689–3702.

Press, W. H., S. A. Teukolsky, W. T. Vetterling, and B. P. Flannery (1992), *Numerical Recipes in C: The Art of Scientific Computing*, 2nd ed., Cambridge Univ. Press, Cambridge, U. K.

Rajaram, R., and S. Gurubaran (1998), Seasonal variabilities of low latitude mesospheric winds, *Ann. Geophys.*, *16*, 197–204.

Rastogi, P. K., K. E. Kudeki, and F. Surucu (1996), Distortion of gravity wave spectra of horizontal winds measured in atmospheric radar experiments, *Radio Sci.*, *1*, 105–118.

Reid, I. M., and R. A. Vincent (1987), Measurement of the horizontal scales and phase velocities of short period mesospheric gravity waves at Adelaide, Australia, *J. Atmos. Terr. Phys.*, *49*, 1033–1048.

Riggin, D., D. C. Fritts, C. D. Fawcett, E. Kudeki, and M. H. Hitchman (1997a), Radar observations of gravity waves over Jicamarca Peru during the CADRE campaign, *J. Geophys. Res.*, *102*, 26,263–26,281.

Riggin, D., D. C. Fritts, T. Tsuda, T. Nakamura, and R. A. Vincent (1997b), Radar observations of a 3-day Kelvin wave in the equatorial mesosphere, *J. Geophys. Res.*, *102*, 26,141–26,157.

Salby, M. L. (1981), Rossby normal modes in the nonuniform background configuration. Part II: Equinox and solstice conditions, *J. Atmos. Sci.*, *38*, 1827–1840.

Salby, M. L., and R. R. Garcia (1987), Transient response to localized episodic heating in the tropics, I. Excitation and short-time near-field behavior, *J. Atmos. Sci.*, *44*, 458–498.

Salby, M. L., D. L. Hartmann, P. L. Bailey, and J. C. Gille (1984), Evidence for equatorial Kelvin modes in Nimbus-7 LIMS, *J. Atmos. Sci.*, *41*, 220–235.

Salby, M. L., H. H. Hendon, K. Woodberry, and K. Tanaka (1991), Analysis of global cloud imagery from multiple satellites, *Bull. Am. Meteorol. Soc.*, *72*, 467–480.

Sato, K. H., and S. Fukao (1995), Gravity waves and turbulence assocaited with cumulus convection observed with UHF/VHF clear-air Doppler radars, *J. Geophys. Res.*, *100*, 7111–7119.

Senft, D. C., and C. S. Gardner (1991), Seasonal variability of gravity wave activity and spectra in the mesopause region at Urbana, *J. Geophys. Res.*, *96*, 17,229–17,264.

Smith, S. A., D. C. Fritts, and T. E. Van Zandt (1987), Evidence for a saturated spectrum of atmospheric gravity waves, *J. Atmos. Sci.*, *44*, 1404–1410.

Sridharan, S., and S. Satish Kumar (2008), Seasonal and interannual variations of gravity wave activity in low-latitude mesopshere and lower thermosphere over Tirunelveli (8.7°N, 77.8°E), *Ann. Geophys.*, *26*, 3215–3223.

Sridharan, S., T. Tsuda, T. Nakamura, R. A. Vincent, and Effendy (2006), Radar observations of 5–8 days wave in the equatorial MLT region, *J. Meteorol. Soc. Jpn.*, *84*, 295–304.

Swenson, G. R., R. Haque, W. Yang, and C. S. Gardener (1999), Momentum and energy fluxes of monochromatic gravity waves observed by an OH imager at Starfire Optical Range, New Mexico, *J. Geophys. Res.*, *104*, 6067–6080.

Thayaparan, T., W. Hocking, and J. MacDougall (1995), Observational evidence of tidal/gravity wave interactions using UW0 2 MHz radar, *Geophys. Res. Lett.*, *22*, 337–376.

Tsuda, T., T. Inoue, D. C. Fritts, T. E. Van Zandt, S. Kato, T. Sato, and S. Fukao (1989), MST radar observations of a saturated gravity wave spectrum, *J. Atmos. Sci.*, *46*, 2440–2447.

Tsuda, T., Y. Murayama, M. Yamamoto, S. Kato, and S. Fukao (1990), Seasonal variation of the momentum flux in the mesosphere observed with the MU radar, *Geophys. Res. Lett.*, *17*, 725–728.

Tsuda, T., Y. Murayama, T. Nakamura, R. A. Vincent, A. H. Manson, C. E. Meek, and R. L. Wilson (1994a), Variations of gravity wave characterstics with height, season and latitude revealed by comparative observations, *J. Atmos. Terr. Phys.*, *56*, 555–568.

Tsuda, T., Y. Murayama, H. Wiryosumarto, S. W. B. Harijono, and S. Kato (1994b), Radiosonde observations of equatorial atmosphere dynamics over Indonesia: 2. characterstics of gravity waves, *J. Geophys. Res.*, *99*, 10,507–10,516.

Tsuda, T., S. Yoshida, T. Nakamura, A. Nuryanto, S. Manurung, O. Sabari, R. A. Vincent, and I. M. Reid (2002), Long-term variations of atmospheric wave activity in the mesosphere and lower thermosphere region over equatorial Pacific, *J. Atmos. Sol. Terr. Phys.*, *64*, 1123–1229.

Tsuda, T., M. V. Ratnam, S. Alexander, T. Kozu, and Y. Takayabu (2009), Temporal and spatial distribution of atmospheric wave energy in the equatorial stratosphere revealed by GPS occulatation temperature data obtained with the CHAMP satellite during 2001–2006, *Earth Planets Space*, *61*, 523–533.

Venkateswara Rao, N., T. Tsuda, S. Gurubaran, Y. Miyoshi, and H. Fujiwara (2011), On the occurrence and variability of the terdiurnal tide in the equatorial mesosphere and lower thermosphere and a comparison with the Kyushu-GCM, *J. Geophys. Res.*, *116*, D02117, doi:10.1029/2010JD014529.

Vincent, R. A., and D. C. Fritts (1987), A climatology of gravity wave motions in the mesopause region at Adelaide, Australia, *J. Atmos. Sci.*, *44*, 748–760.

Vincent, R. A., and D. Lesicar (1991), Dynamics of the equatorial mesosphere: First results with a new generation partial reflection radar, *Geophys. Res. Lett.*, *18*, 825–828.

Vincent, R. A., A. MacKinnon, I. M. Reid, and M. J. Alexander (2004), VHF profiler observations of winds and waves in the troposphere during the Darwin Area Wave Experiment (DAWEX), *J. Geophys. Res.*, *109*, D20S02, doi:10.1029/2004JD004714.

Vincent, R. A., S. Kovalam, I. M. Reid, and J. P. Younger (2010), Gravity wave flux retrievals using meteor radars, *Geophys. Res. Lett.*, *37*, L14802, doi:10.1029/2010GL044086.

Wang, D. Y., and D. C. Fritts (1990), Mesospheric momentum fluxes observed by the MST radar at Poker Flat, Alaska, *J. Atmos. Sci.*, *47*, 1512–1521.

Wheeler, M., and G. N. Kildas (1999), Convectively coupled equatorial waves: Analysis of clouds and temperatures in the wavenumber-frequency domain, *J. Atmos. Sci.*, *56*, 374–399.

Yoshida, S., T. Tsuda, A. Shimizu, and T. Nakamura (1999), Seasonal variations of 3.0~3.5 day ultra fast Kelvin waves observed with a meteor radar and radiosondes in Indonesia, *Earth Planets Space*, *51*, 675–684.

S. Gurubaran, Equatorial Geophysical Research Laboratory, Indian Institute of Geomagnetism, Tirunelveli, India. (gurubara@iigs.iigm.res.in)

S. Kovalam, School of Physics and Chemistry, University of Adelaide, North Terrace, Adelaide, SA 5005, Australia. (sujata.kovalam@adelaide.edu.au)

T. Tsuda, Research Institute for Sustainable Humanosphere, Kyoto University, Uji, Japan. (t.tsuda@rish-kyoto.jp)